

# Sweeping echoes perceived in a regularly shaped reverberation room

Kenji Kiyohara<sup>a)</sup> and Ken'ichi Furuya

*NTT Cyber Space Laboratories, 3-9-11 Midori-cho, Musashino-shi, Tokyo 180-8585, Japan*

Yutaka Kaneda

*Tokyo Denki University, 2-2 Kanda-Nishiki-cho, Chiyoda-ku, Tokyo 101-8457, Japan*

(Received 15 January 2001; revised 30 October 2001; accepted 12 November 2001)

A very interesting new phenomenon that we call a sweeping echo is described and investigated. When we clap hands in a regularly shaped reverberant room, we hear sweeping echoes whose frequency increases linearly with time. An example of sweeping echoes observed in a rectangular reverberation room is first described. Then, the mechanism that generated the sweeping echoes is investigated by assuming a cubic room and using number theory. The reflected pulse sound train is found to have almost equal intervals between pulses on the squared-time axis. This regularity of arrival times of the reflected pulse sounds is shown to generate the sweeping echoes. Computer simulation of room acoustics shows good agreement with the theoretical results. © 2002 Acoustical Society of America. [DOI: 10.1121/1.1433808]

PACS numbers: 43.55.Br, 43.55.Ka, 43.20.El [JDQ]

## I. INTRODUCTION

A new, interesting acoustical phenomenon is described, and its generation mechanism is investigated theoretically.

When we clap hands once between parallel, hard walls, we hear a sound called a “fluttering echo.”<sup>1</sup> A single hand clap sound (i.e., an impulsive sound) is reflected by the walls repeatedly, and a train of pulses with periodic intervals is generated. This pulse train causes a specific sound sensation; that is, a fluttering echo.

In the fluttering echo, reflected sounds go forward and backward in a one-dimensional pattern between parallel hard walls. What happens, then, when we clap hands in a three-dimensional reflective space? We found that sweep sound (Audio illustrations are available at: <http://www.asp.c.dendai.ac.jp/sweep/> and <http://www.ntt.co.jp/cclab/info/sweep.html>) which we call “sweeping echoes,” were perceived when we generated a pulse sound in a regularly shaped reverberation room. The perceived frequencies of the sweep sounds increased with time at different speeds. Other researchers have also noticed the sweeping echoes in squash courts, which also had hard regularly shaped walls.

There are some other types of sweeping (or sliding) echoes. One is caused by frequency dispersion. The frequency dispersion assumes some special sound field where the phase velocity of a sound varies with its frequency. This is not the case here; the sweeping echoes presented in this paper occur in a normal sound field, without dispersion.

Knudsen<sup>2</sup> reported another type of frequency shift in reverberated sound. He reported that the pitch of a tone in a small, resonant room might change perceptibly during the decay of the tone. The pitch of the emitted sound is considered to be changed to that of a resonance frequency. On the other hand, our sweeping echoes are clearly explained in the time domain based on the number theory.

In this paper, the sweeping echoes observed in a rectangular parallelepiped reverberation room are described first with their time-frequency analysis in Sec. II. Then, the generation mechanism of the sweeping echoes in a cubic room is investigated using number theory in Secs. III and IV. The theoretical results are compared with simulation results in Sec. V. Sweeping echoes in a rectangular parallelepiped room are discussed in Sec. VI and Sec. VII concludes the paper.

## II. SWEEPING ECHOES PERCEIVED IN A RECTANGULAR PARALLELEPIPED REVERBERATION ROOM

Sweeping echoes are perceived in relatively large, regularly shaped three-dimensional rooms with highly reflective surfaces; i.e., walls, ceiling, and floor. We first describe the sweeping echoes measured in a rectangular parallelepiped reverberation room along with their time-frequency analysis.

### A. Measurement conditions and sweeping echoes

The dimensions of the rectangular parallelepiped reverberation room were 11 m (width) × 8.8 m (depth) × 6.6 m (height).<sup>3</sup> The measurement conditions are shown in Fig. 1. Figures 1(a) and (b) show the plan view and cross section of the reverberation room, respectively. The symbols *S* and *R* represent the source and reception positions, respectively. As shown in Fig. 1(a), both *S* and *R* were located on the center line of the floor. *S* was located 3.2 m from the wall and 1.2 m high, and *R* was 1.1 m from the opposite wall and 1.5 m high as shown in the figure, respectively.

When hands were clapped once at position *S*, the first sweep sound whose frequency increased over a short time (called the main sweeping echo) was perceived at position *R*. Multiple sweep sounds whose frequency increased relatively slowly (called subsweeping echoes) were then perceived, along with ordinary reverberation sounds.

<sup>a)</sup>Electronic mail: kiyohara.kenji@lab.ntt.co.jp

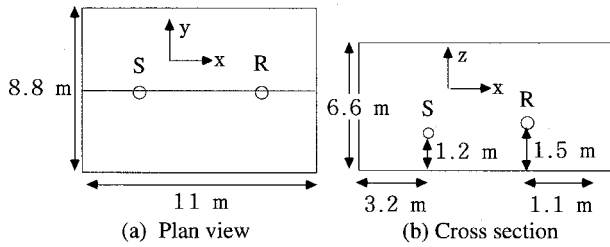


FIG. 1. Layout for sweep-sound measurement. (a) Plan view, (b) cross section,  $S$ , source position,  $R$ , reception position.

Although sweep sounds were perceived at other source and reception positions, the sounds were perceived more clearly at positions that were symmetrical with respect to the room, such as those shown in Fig. 1. To analyze these sweep sounds, they were recorded with a microphone placed at position  $R$ .

## B. Time-frequency analysis of the sweeping echoes

Figure 2 shows the results of analyzing the recorded echoes by using short-time Fourier transformation. The horizontal axis represents time, and the time when hands were clapped is set to the origin. The figure shows the spectrogram for the first 2 seconds. The vertical axis represents frequency, up to 2 kHz, which was the range within which the sweep sounds were clearly perceived. The analysis conditions were the following: the sampling frequency was 16 kHz, a 16-ms rectangular window (62.5 Hz frequency resolution) was used, and the window was shifted in steps of 8 ms.

In Fig. 2, the main sweeping echo appears clearly from 0 to about 400 ms [line (A)]. The frequency of the main sweeping echo increased linearly with time, and it rose to about 1500 Hz during the first 400 ms. This result corresponds with hearing perception. Following the main sweeping echo, multiple subsweeping echoes whose frequencies rose linearly at relatively slow speeds, also appear in Fig. 2.

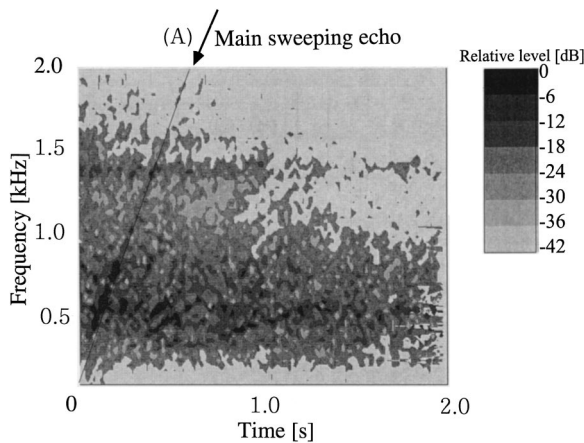


FIG. 2. Spectrogram of the recorded data. The main sweeping echo appears clearly from 0 to about 400 ms [line (A)]. The frequency of the main sweeping echo increased linearly with time, and it rose to about 1500 Hz during the first 400 ms. Following the main sweeping echo, multiple subsweeping echoes also appeared whose frequency rose linearly at relatively slow speeds.

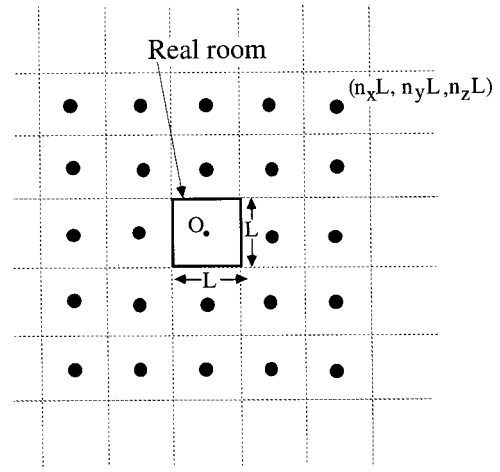


FIG. 3. Mirror image sources of a cubic room. The figure shows a top view, and the size of the room is denoted by  $L$ . The reflected sounds are treated as the sounds from the image sources. The coordinate origin  $O$  is set to the center of the room. The location of each image source is represented by  $(n_x L, n_y L, n_z L)$  where  $n_x, n_y, n_z$  are positive and negative integers.

## III. GENERATION MECHANISM OF THE MAIN SWEEPING ECHO

In this section, we investigate the generation mechanism of the main sweeping echo, based on geometrical acoustics and number theory. As the first step in this investigation, a cubic room is assumed in this paper.

### A. Intervals of reflected sounds in a cubic room

First, the regularity of arrival time of reflected sounds in a cubic room is described. To simplify the issue, the source and reception points are both assumed to be located at the center of the room. Figure 3 shows the mirror image sources generated in a cubic room based on geometrical acoustics.<sup>4</sup> The figure shows a top view, and the edge length of the room is denoted by  $L$ . When a pulse sound is generated at the center of the room, the arrival times and amplitudes of the observed reflected sounds are the same as those of the sounds that would be generated from the image sources shown in Fig. 3. In other words, the reflected sounds can be treated as the sounds from the image sources.

The coordinate origin  $O$  is set at the center of the room. Then, the location of each image source is represented by  $(n_x L, n_y L, n_z L)$ , where  $n_x, n_y, n_z$  are integers. The distance  $d$  between the origin (reception position) and an image source of  $(n_x L, n_y L, n_z L)$  is represented by

$$d = \sqrt{(n_x L)^2 + (n_y L)^2 + (n_z L)^2} = \sqrt{n_x^2 + n_y^2 + n_z^2} \cdot L. \quad (1)$$

Thus, the arrival time of the sound from the image source is obtained by dividing  $d$  by the sound velocity  $c$ , as in the following equation:

$$t = d/c = \sqrt{n_x^2 + n_y^2 + n_z^2} \left( \frac{L}{c} \right). \quad (2)$$

Next, consider the arrival time on the squared-time axis. The squared arrival time is derived by squaring Eq. (2):

$$t^2 = (n_x^2 + n_y^2 + n_z^2) \left( \frac{L}{c} \right)^2 = M \left( \frac{L}{c} \right)^2, \quad (3)$$

where

$$M = n_x^2 + n_y^2 + n_z^2. \quad (4)$$

Thus, the squared arrival time  $t^2$  is represented by an integer  $M$  times a constant  $(L/c)^2$ . Equation (3) represents the position on the squared-time axis at which the reflected sound exists.

From number theory,<sup>5</sup> the sum of the squared integers  $(n_x^2 + n_y^2 + n_z^2)$  expresses all integers, except the “forbidden numbers,” i.e.,

$$M \neq 4^k(8m + 7), \quad (5)$$

where  $k, m = 0, 1, 2, \dots$

Since these forbidden numbers account for 1/6 of all positive integers, we first disregard the forbidden numbers and assume that  $M$  includes approximately all positive integers. Then, Eq. (3) indicates that reflected sounds (pulse sounds) exist at  $(L/c)^2, 2(L/c)^2, 3(L/c)^2, \dots$ ; that is, they exist at equal intervals of  $(L/c)^2$  on the squared-time axis.

### B. Relationship between the squared-time axis and the time axis

We represent the arrival times of two adjacent pulses (reflected sounds) as  $t_a$  and  $t_b$  ( $t_a < t_b$ ). The interval between these pulses on the squared-time axis is  $(L/c)^2$ . Namely

$$t_b^2 - t_a^2 = \left(\frac{L}{c}\right)^2. \quad (6)$$

By factoring the left-hand side of Eq. (6), we obtain

$$(t_b - t_a)(t_b + t_a) = \left(\frac{L}{c}\right)^2. \quad (7)$$

The average arrival time  $t_v$  of the two pulses is defined by

$$t_v = (t_b + t_a)/2. \quad (8)$$

By substituting Eq. (8) into Eq. (7) and modifying it, the interval between pulses on the time axis is represented by the following equation:

$$t_b - t_a = \left(\frac{L^2}{2c^2}\right) \left(\frac{1}{t_v}\right). \quad (9)$$

Equation (9) clarifies that the interval between the two pulses is inversely proportional to the time  $t_v$ .

Thus, a pulse series with equal intervals on the squared-time axis has intervals inversely proportional to time on the time axis. Figure 4 illustrates this relationship.

### C. Main sweeping echo

A periodic pulse series has a fundamental frequency represented by the reciprocal of its interval.<sup>6</sup> Therefore, when the interval of pulses is represented by Eq. (9), the fundamental frequency of the pulses at time  $t_v$  is expressed by the following equation:

$$f(t_v) = \frac{1}{t_b - t_a} = \left(\frac{2c^2}{L^2}\right) t_v. \quad (10)$$

Equation (10) indicates that the fundamental frequency  $f$  is proportional to the time  $t_v$ . In other words, humans perceive

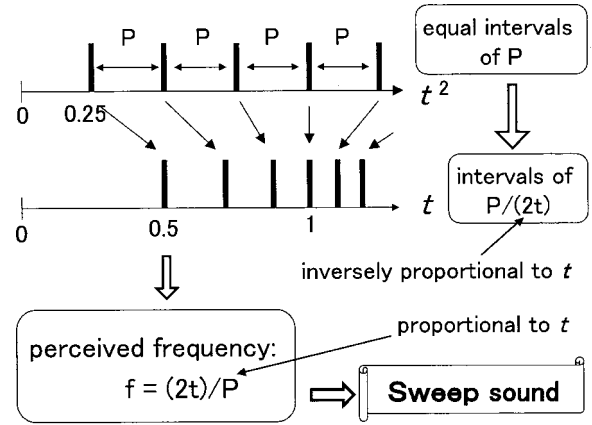


FIG. 4. A pulse series with equal intervals on the squared-time axis has intervals inversely proportional to time on the time axis.

an increasing sweep sound. This proves that a reflective pulse train in a cubic room produces a sweep sound sensation.

### IV. GENERATION MECHANISM OF THE SUBSWEEPING ECHOES (INFLUENCE OF THE FORBIDDEN NUMBERS)

As described above, a pulse series from the image sources of a cubic room does not have completely equal intervals on the squared-time axis because of the forbidden numbers. The influence of the forbidden numbers can be explained as the addition of a forbidden numbers pulse train which has pulses corresponding to forbidden numbers on the squared-time axis with negative amplitudes. Figure 5 conceptually illustrates this phenomenon. Figure 5(a) shows a pulse series on the time axis of a cubic room for equal amplitudes, where the dimension  $L$  of the cubic room was assumed to be 10 m. Some pulses are missing because of the

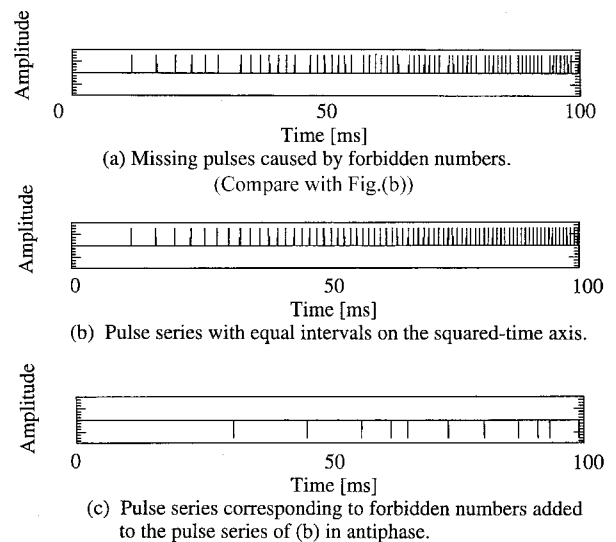


FIG. 5. The influence of the forbidden numbers. (a) A pulse series on the time axis of a cubic room for equal amplitudes. (b) A pulse series with completely equal intervals on the squared-time axis. (c) A pulse series corresponding to the forbidden numbers with the negative amplitude of the same values. The gaps of (a) are considered to be generated by adding (c) to (b), where the dimension  $L$  of the cubic room was assumed to be 10 nm.

forbidden numbers. These gaps were considered to be generated by adding a pulse series corresponding to the forbidden numbers with negative amplitude of the same values [Fig. 5(c)] to a pulse series with completely equal intervals on the squared-time axis [Fig. 5(b)].

From Eqs. (3) and (5), the squared arrival time for the pulse series corresponding to the forbidden numbers is represented by the following equation:

$$t^2 = 4^k(8m+7)\left(\frac{L}{c}\right)^2, \quad (11)$$

where  $k, m = 0, 1, 2, 3, \dots$

The pulse series has equal intervals of  $4^k 8(L/c)^2$ , for  $k = 0, 1, 2, \dots$ , on the squared-time axis as  $m$  changes. For a typical example, corresponding to  $k = 0$  and  $m = 0, 1, 2, \dots$ , the period of the pulse series becomes  $8(L/c)^2$ . The fundamental frequency at the mean time  $t_v$  of two adjacent pulses corresponding to this example is represented by the following equation:

$$f_b(t_v) = \left(\frac{2c^2}{L^2}\right) \frac{1}{8} t_v. \quad (12)$$

For  $k = 1$  and  $m = 0, 1, 2, \dots$ , the period of the pulses becomes  $32(L/c)^2$ , and its fundamental frequency is represented by the following equation:

$$f_b(t_v) = \left(\frac{2c^2}{L^2}\right) \frac{1}{32} t_v. \quad (13)$$

For  $k = 2, 3, 4, \dots$ , the fundamental frequency is represented in a similar way.

The pulses series corresponding to the forbidden numbers thus consists of multiple pulse series with different periods on the squared-time axis. Since these periods are longer than that of the main sweeping echo, the fundamental frequencies of the pulse series corresponding to the forbidden numbers increase more slowly. Thus, subsweeping echoes are generated.

## V. NUMERICAL SIMULATION

The theoretical results derived in the preceding sections were confirmed by time-frequency analysis. Figure 6(a) shows the spectrogram of the pulse series shown in Fig. 5(b). The spectrogram was calculated by FFT with a 16-ms rectangular time window and an 8-ms shift. In Fig. 6(a), the main sweeping echo (A) appears clearly. The lines (B) are its harmonics. Calculating the slope (or frequency rising speed, or sweep speed) of the main sweeping echo from Eq. (10) with sound velocity  $c = 340$  m/s gave  $2c^2/L^2 = 2312$  Hz/s. This value is consistent with the slope of the main sweeping echo (A) shown in Fig. 6(a).

Figure 6(b) shows the spectrogram of the pulse series shown in Fig. 5(c). The subsweeping echo (C) corresponding to  $k = 0$  appears clearly, and its harmonics (D) also appear. Calculating the slope of the subsweeping echo for  $k = 0$  from Eq. (12) gave  $(2c^2/L^2)/8 = 289$  Hz/s. This value is consistent with the slope of the subsweeping echo (C) shown in Fig. 6(c).

Figure 7 shows the spectrogram of the pulse series

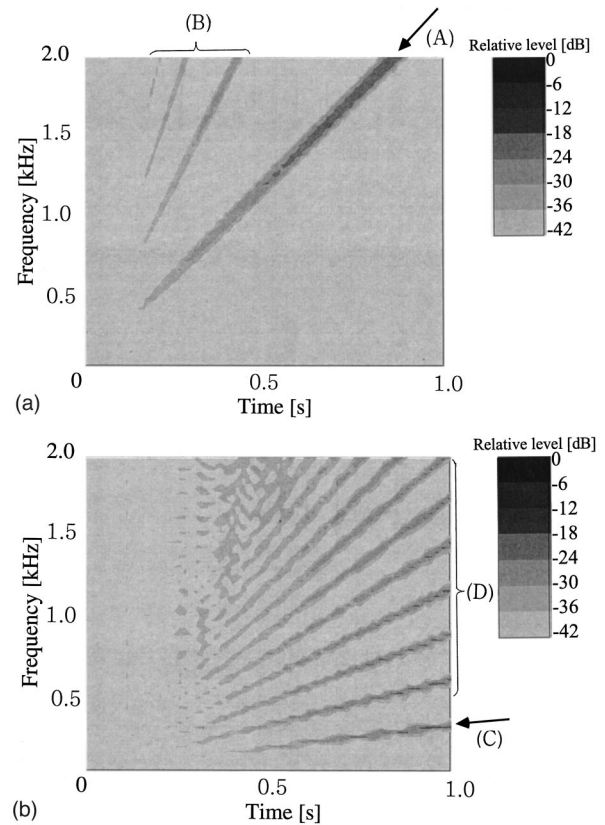


FIG. 6. (a) Spectrogram of the pulse series shown in Fig. 5(b). The main sweeping echo (A) appears clearly. The lines (B) are its harmonics. (b) Spectrogram of the pulse series shown in Fig. 5(c). The subsweeping echo (C) appears clearly, and its harmonics (D) also appear.

shown in Fig. 5(a). The spectrogram is almost the power sum of the spectra shown in Figs. 6(a) and (b). The main sweeping echo (A) and its harmonics (B), and the subsweeping echo (C) corresponding to  $k = 0$  and its harmonics (D) all appear in Fig. 7. Thus, the main sweeping echo and the subsweeping echoes corresponding to the forbidden numbers were perceived for the pulse series shown in Fig. 5(a).

Next, the reflected sounds of a pulse sound (i.e., an impulse response) in the cubic room were simulated by the

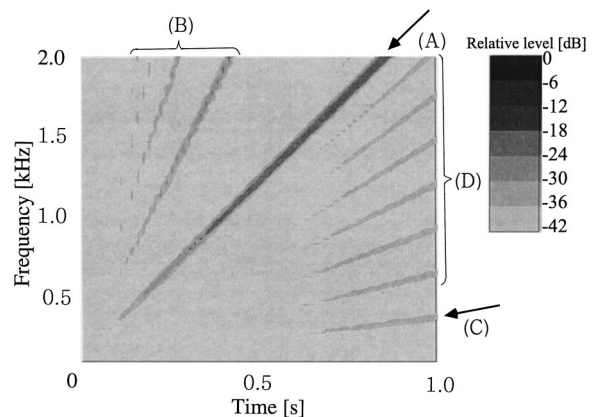


FIG. 7. Spectrogram of the pulse series shown in Fig. 5(a). The spectrogram is almost the power sum of the spectra shown in Figs. 6(a) and (b). The main sweeping echo (A) and its harmonics (B), and the subsweeping echo (C) and its harmonics (D) all appear.

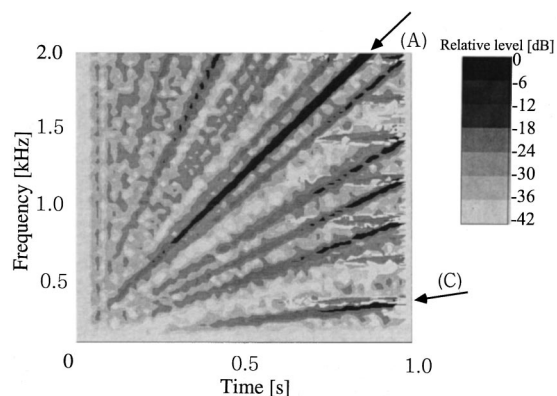


FIG. 8. Spectrogram of the impulse response in a cubic reverberation room whose dimension  $L$  is 10 m. Multiple sweep sounds appear, and just as in Fig. 7, the main sweeping echo (A) appear clearly. The subsweeping echo (C) also appears.

mirror image source method.<sup>7</sup> Dimension  $L$  for the room was 10 m. The calculated reflected pulses were convolved with a sinc function and overlap added<sup>8</sup> to derive sampling data. Figure 8 shows the spectrogram of the simulated sounds. Multiple sweep sounds appear, and just as in Fig. 7, the main sweeping echo (A) appears clearly. The subsweeping echo (C) also appears.

Since the sound source and reception point were located at the center of the room, different numbers of multiply reflected pulses arrived at the same time due to the degeneracy of the mirror image sources. Therefore, the amplitudes of the reflected-pulse series were not equal. This caused the random noisy spectrum that was superposed on the time-spectrum plot. As a result, the sweeping echoes shown in Fig. 8 are somewhat obscure. However, the same sweeping echoes shown in Fig. 7 can also be recognized in Fig. 8.

The slopes of lines (A) and (C) in Fig. 8 are similar to the theoretical values 2312 Hz/s and 289 Hz/s, respectively, calculated above. Thus, the theoretical results developed in the preceding section adequately explain the sweeping echo phenomenon that appeared in the computer simulation of room acoustics.

## VI. RECTANGULAR PARALLELEPIPED REVERBERATION ROOM

Unlike a cubic room, all the side lengths of a rectangular parallelepiped room are not equal. Therefore, the arrival time of a reflected sound from an image source cannot be represented by a simple formula like Eq. (2). This makes theoretical analysis using number theory difficult.

Therefore, we attempted a qualitative explanation by analyzing experimental data. A pulse sound was generated by hand clapping under the conditions shown in Fig. 1. Then, the periodicity of the received pulse train (reverberation sound) was studied based on the short-time autocorrelation method. The short-time autocorrelation function  $\rho(\tau, t_w)$  was calculated from the windowed data centered at time  $t_w$ , and it was calculated repeatedly with sliding time  $t_w$ . The sampling frequency was 16 kHz, and the window length was 10 ms.

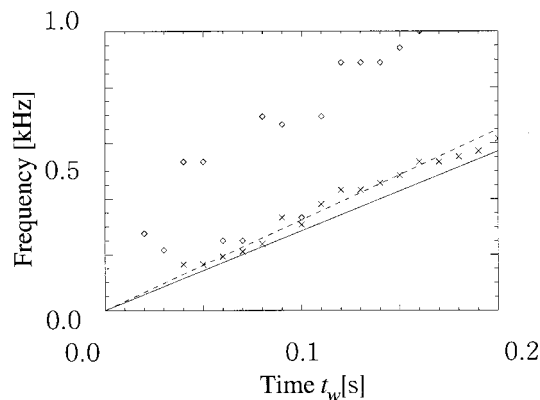


FIG. 9. Reciprocal of peak time of short-time autocorrelation  $\rho(\tau)$  of recorded data shown in Fig. 2.  $\diamond$ , the first high peak of  $\rho(\tau)$ .  $\times$ , the second high peak of  $\rho(\tau)$ . Solid line, theoretical frequency. The solid line is close to the  $\times$  symbols. Broken line, the line of main sweeping echo observed in Fig. 2. It is also close to the theoretical line plot.

When the reflected pulses contain periodic pulses, the autocorrelation function  $\rho(\tau, t_w)$ , as a function of time  $\tau$  with fixed  $t_w$ , has peaks at times,  $\tau$  s, corresponding to the pulse periods. These peak times, or pulse periods were calculated as a function of  $t_w$ . The results are shown in Fig. 9, as the reciprocals of the detected periods, which correspond to the frequencies.

In Fig. 9, the horizontal axis represents the time  $t_w$  and the vertical axis represents the reciprocal of the peak of the autocorrelation function by frequency. The  $\diamond$  symbol denotes the frequencies that correspond to the first high peaks of  $\rho(\tau, t_w)$  for each  $t_w$ , and the  $\times$  symbol denotes the frequencies that correspond to the second high peaks.

The root-mean-square  $L_m$  of the side lengths of the rectangular parallelepiped room was calculated using the following equation:

$$L_m = \sqrt{(L_x^2 + L_y^2 + L_z^2)}/3. \quad (14)$$

Substituting the dimension of the experimental room ( $L_x = 11$  m,  $L_y = 8.8$  m,  $L_z = 6.6$  m from Fig. 1) gave  $L_m = 8.98$  m. A function derived by substituting  $L_m$  into Eq. (10), representing the theoretical frequency of a main sweeping echo for a cubic room with side length of  $L_m$ , is shown as a solid line in Fig. 9. This solid line is close to the  $\times$ . The line of the main sweeping echo observed in Fig. 2 is also plotted in Fig. 9, by a broken line, and it is also close to the theoretical line plot.

This result indicates that the calculated frequency line of a sweeping echo based on  $L_m$  matches the observed sweeping echo, and its sweeping frequency corresponds to the periodicity in the pulse train appearing as the second high peak of the short-time autocorrelation function. It is left for future study to answer the questions why the second high peaks but not the first ones, and what do the first high peaks represent.

Thus, the main sweeping echo in a rectangular parallelepiped room has reflected pulse periods close to those of a cubic room with the same mean side length  $L_m$  as the rectangular parallelepiped room. This implies that the pulse train

in a rectangular parallelepiped room has a regularity similar to that in a cubic room, and this regularity causes sweeping sounds.

## VII. CONCLUSION

When a pulse sound is generated in a rectangular parallelepiped reverberation room, a peculiar phenomenon is observed in that the frequency components of the reflected sounds increase linearly (called “sweeping echoes”). These sweeping echoes consist of a “main sweeping echo,” whose frequency component increases over a short time, and “sub-sweeping echoes,” whose frequency components increase slowly. Investigating the sweeping echoes assuming a cubic room showed that the arrival times of the pulse sounds from mirror image sources had almost equal intervals on the squared-time axis, and this regularity of the pulse intervals generated the main sweeping echo. The pulse train does not have exactly equal intervals on the squared-time axis, but rather has some missing pulses corresponding to “forbidden numbers” based on number theory. These missing pulses were shown to have relatively long, equal intervals. This regularity causes the subsweeping echoes. Computer simulation based on the image method produced results in good agreement with the theoretical results.

## ACKNOWLEDGMENTS

We thank Kazuhiko Yamamori, Dr. Nobuhiko Kitawaki, and Junji Kojima for their support of our work. We thank Masashi Tanaka for his useful advice. We thank our colleagues for their help in measuring the sounds.

<sup>1</sup>E. Meyer and E.-G. Neumann, *Physical and Applied Acoustics* (Academic, New York, 1972), pp. 92–94.

<sup>2</sup>V. O. Knudsen, “Resonance in small rooms,” *J. Acoust. Soc. Am.* **3**, 20–37 (1932).

<sup>3</sup>M. Tohyama and S. Yoshikawa, “Approximate formula of the averaged sound energy decay curve in a rectangular reverberant room,” *J. Acoust. Soc. Am.* **70**, 1674–1678 (1981).

<sup>4</sup>H. Kuttruff, *Room Acoustics* (Elsevier Applied Science, London, 1991), pp. 81–95.

<sup>5</sup>M. R. Schroeder, *Number Theory in Science and Communication* (Springer-Verlag, Berlin, 1984), pp. 97–99.

<sup>6</sup>A. Papoulis, *The Fourier Integral and Its Application* (McGraw-Hill, New York, 1962), pp. 43–44.

<sup>7</sup>J. B. Allen and D. A. Berkley, “Image method for efficiently simulating small-room acoustics,” *J. Acoust. Soc. Am.* **65**, 943–950 (1979).

<sup>8</sup>A. V. Oppenheim and R. W. Schaffer, *Digital Signal Processing* (Prentice-Hall, New Jersey, 1975), pp. 26–30.